INVESTIGATING SUB-RESOLUTION SURFACE PROPERTIES OF COMET 67P/CHURYUMOV-GERASIMENKO FROM OPTICAL PHOTOMETRY AND HAPKE MODELING.

S.A. Moruzzi[1,2], A.G. Hayes[1], J.M. Soderblom[3], P. Corlies[3] , S.P.D. Birch[3], N.W. Kutsop[1], P. Helfenstein[1]. [1]Cornell University, Ithaca, NY [2]University of Arizona, Tuscon, AZ (smoruzzi@email.arizona.edu) [3]MIT, Cambridge, MA

Introduction: Observations from the Rosetta spacecraft's Optical, Spectroscopic, and Infrared Imaging System (OSIRIS) Narrow Angle Camera (NAC) of Comet 67P/Churyumov-Gerasimenko (67P) have provided the high resolution images of a cometary surface at multiple observation geometries. The dataset has revealed that the surface is dominated by smooth plains, cauliflower plains, pitted plain, and consolidated terrains [1-3]. In this study, we present multispectral phase curves between 0° and 160° in 10 filters for type examples of each primarily morphologic unit. We fit these phase curves to Hapke, (2012) photometric functions [4] to derive photometric properties including single scattering albedo and macroscopic roughness. Results are compared to previously published best-fit Hapke coefficients of disk-integrated reflectance [5,7].

Our results are consistent with the qualitative interpretation that the smooth plains are the photogeologically smoothest of the four regions with the highest albedo and the consolidated terrains are the photogeologically roughest terrains with the lowest albedo (hereafter "smooth" and "rough" terrains respectively). Macroscopic roughness tends to be correlated with other photometric properties in each terrain. Aspects including parameter trends across wavelengths, type-examples within single morphologies, between different terrain types, and against disk-integrated models are indicative of variable levels of erosional and active processes. We discuss these results in the context of their importance to the surface properties of 67P.

Method: Rosetta's OSIRIS NAC images, taken in wavelengths ranging from ~200-1000 nm, revealed a diverse and evolving landscape across the surface of the comet, showing two broad terrain categories: smooth terrains and rough terrains [1]. Smooth terrains consist of small, granular material that is hypothesized to have been previously consolidated bedrock. These terrains include smooth, pitted, and cauliflower plains. In contrast, consolidated terrains (low reflectance [5,7]) consist of the exposed comet nuclei, or bedrock, including cliff terrains [1].

We have chosen four morphologies, as defined by [1], for this study and aim to quantitatively distinguish between them. Three of the four representative sites that were chosen are examples of smooth terrain: smooth plains in the Imhotep region, cauliflower plains in the Ash region and pitted plains in the Ma'at region. The fourth site is an example of consolidated terrain, located in the Agilkia (or Abydos) region. We use the SPICE toolkit from NAIF (Navigation and Ancillary Information Facility, [6]) to generate navigation information for each pixel and determine the relevant incidence, emission, and phase angles.

For each of the selected sites, we chose a representative image and manually selected a region of interest. The navigation information for all of the pixels within each region of interest (<1 m pixel scale were used to create the phase curves (I/F radiance factors vs. phase angle). Resulting phase functions were also compared with disk integrated models derived by [7, 8].

We utilized the reflectance function from [4] that includes macroscopic roughness to fit our phase curves and in doing so, determine our best fit "Hapke parameters": single scattering albedo (ω), an asymmetry parameter for the Henyey-Greenstein Function (ξ), the coefficient of the shadow-hiding opposition effect function (B_{S0}), internal parameter shadow hiding opposition effect function parameter (h_s) and macroscopic roughness (θ). We use a Levenberg-Marquardt curve fitting routine and 1000-run Monte Carlo simulations to search within specified ranges of these parameters for the best fit values for the observed phase curve. The ranges we tested include ω = 0.01-1, ξ = -0.75-0.75, B_{S0}= 0-1, h_s = 0-0.75 and θ = 0-40°. We did not derive best fitting values for the coherent backscattering parameter (B_{C0}) nor the coefficient for (h_c) because our dataset was not sensitive to these parameters (insufficient low incidence observations). An empirical correction accounting for interfacet multiple scattering in the macroscopic roughness term was employed but had a minor effect on our results due to the consistently low single scattering albedo across wavelengths [4]. As an estimated error for parameters weighting, we binned pixels within similar observational geometry (within 0.X°) and determining the standard deviation in each bin.

Results: The shape of both observed and modeled phase curves for morphologies in the "smooth" terrain classification show a steep slope with the highest I/F values at low phase, while curves for consolidated terrains have a flatter slope with lower I/F values near low phase (Fig. 1), as expected. Consolidated terrains lack low phase angles so we cannot constrain B_{S0} and h_s. For this reason, we did not include these parameters in the fitting routine for consolidated terrains.

Our results shows that single scattering albedo decreases within the "smooth" terrain classification and is at a minimum for consolidated terrains. We expect the ξ parameter to increase with microscopically (smaller than the wavelength) rougher terrain, which occurs in most but not all filters. All asymmetry parameters for all morphologies are less than zero, suggesting a preference for backscattering. The asymmetry parameter for the consolidated terrain is closest to isotropic scattering (ξ~0) in

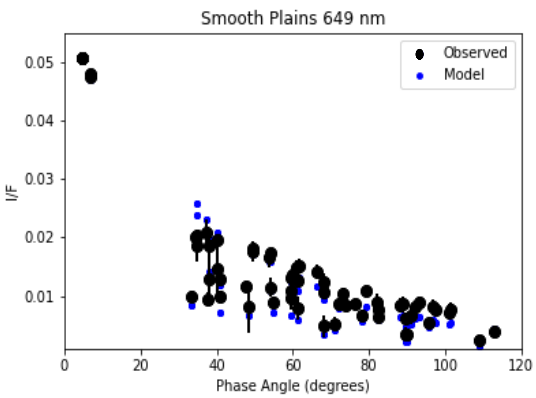

Figure 1: **Observed phase curve (black) compared to the best fitting modeled [4] phase function. Both curves are steeper at low phase angles.**

comparison to the other three morphologies of interest. The B_{S0} for all morphologies of interest within the smooth terrain classification is ~ 0.99-1, which is the physical upper limit of our range for this parameter. While we were able to constrain this parameter within the smooth terrain classification, these sites had minimal low phase data, which could explain why the best fit is the upper limit.. The h_s, parameter is the coefficient for the shadow-hiding backscattering opposition effect or the width of that function and is expected to be anti-correlated with B_{S0}.

Our final parameter, θ, is the macroscopic roughness of a particular surface, or the mean slope angle of areas of the surface that are larger than the particle size but smaller than the detector footprint [4]. Macroscopic roughness should generally increase with increasing surface roughness, but it depends on the size of the facets in the area of interest. Terrains consisting of smaller particles may have larger slope facets between the particles than larger, flat facets in fractured terrain [9]. Our best fit values for this parameter are positively correlated with single scattering albedo and our asymmetry parameter (Fig. 2).

We see a generally increasing trend of single scattering albedo with wavelength for all morphologies, which could be indicative of changes in particle size. There is no distinguishable trend for the asymmetry parameter across wavelengths. The asymmetry parameters and albedo of the cauliflower terrain are similar, to within error, to the disk-integrated values suggesting that cauliflower terrains contributed heavily to the disk-integrated values [7].

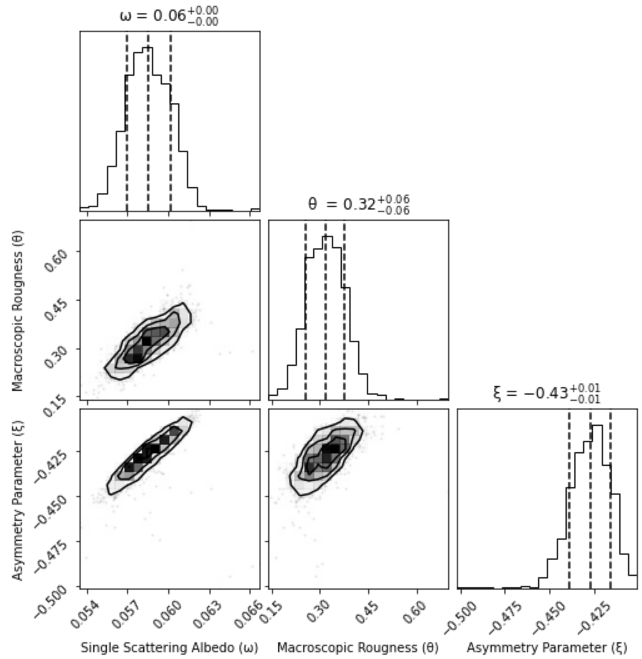

Figure 2**: Correlations between single scattering albedo, asymmetry parameter and macroscopic roughness parameters for the Smooth Plains morphology in the 649 nm filter. Error ellipses show the best fit value for each parameter in the center and uncertainties of 1-σ rounded to two significant figures are reported.**

In summary, our photometric analysis of Comet 67P has shown that we can quantitatively distinguish the different morphologies from one another and that we cannot only quantitatively differentiate the smooth terrains from the consolidated terrains, but also differentiate the morphologies within the smooth terrain classification.. Photometric analysis of additional sites for selected terrain types show similar results to the ones presented here. Finally, even though we can constrain the macroscopic roughness parameter, the analysis provides insight into the facets that govern photometry in these morphologies.

References: [**1**] Birch, et al., (2017), S50-S67. [**2**] El-Maary, et al, (2019) *Space Science Reviews*, 215(4), 36. [**3**] Thomas, et al., (2015), *Science*, S*47*(6220), aaa0440. [**4**] Hapke, (2012), Cambridge University Press. [**5**] Cappacioni, et.al., (2015) *Science, 347* (6220), aaa0628. **[6]** Acton, et.al., (2018), Planetary and Space Sciences, 150, 9-12. [**7**] Fornasier, et al., (2015) *Astronomy & Astrophysics, 583,* A30. [**8**] Ciarniello M. et al., 2015, A&A, 583, A31. [**9**] Shepard and Helfenstein., (2007) *JGR: Planets*, 112(E3).